On the Problems of Symbol-Spaced Tapped-Delay-Line Models for WSSUS Channels*

Carlos A. Gutiérrez[†‡] Margarita Cabrera-Bean[§] Matthias Pätzold[†]

17th February 2008

Abstract

This paper analyzes the pertinence and statistical behavior of symbol-spaced tapped-delay-line (SSTDL) models for wide-sense stationary uncorrelated scattering (WSSUS) mobile radio channels. SSTDL models are obtained by sampling the channel impulse response (CIR) in delay domain at a rate equal to the reciprocal of the symbol duration. They were proposed more than four decades ago as canonical channel models for band-limited time-variant linear systems, and are nowadays widely in use for assessing the performance of several wireless communication systems. The applicability of these tapped-delay-line (TDL) models seems to be unquestionable, as they were developed in the framework of the sampling theorem. Nonetheless, we show here that SSTDL models should be used with care to model WSSUS channels, because the channel's uncorrelated scattering (US) condition might easily be violated. Furthermore, we show that SSTDL models suffer from strong limitations in emulating the channel frequency correlation function (FCF). This drawback leads to an inaccurate performance evaluation of wireless communication systems sensitive to the FCF. To cope with this problem, we present a simple solution by doubling the channel's sampling rate. The benefits of this solution are demonstrated with some exemplary simulation results.

Keywords—Frequency correlation function, multipath channel, sampling theorem, time-variant linear systems, tapped-delay-line model, WSSUS model.

*This work was financed in part by the Catalan Ministry for Universities, Research and the Information Society, and by the Spanish/Catalan Science and Technology Commissions and FEDER funds from the European Commission: TEC2006-06481/TCM, TEC2004-04526, TIC2003-05482, and 2005SGR-00639.

[†]Faculty of Engineering and Science, Department of Information and Communication Technology, University of Agder, Grooseveien 36, NO-4876 Grimstad, Norway.

[‡]Correspondance to: C. A. Gutiérrez. E-mail: carlos.a.gutierrez@uia.no.

[§]Signal Theory and Communications Department, Polytechnic University of Catalonia, Campus Nord UPC D-5, C/Jordi Girona 1-3, 08034 Barcelona, Spain.

1 Introduction

The wide-sense stationary uncorrelated scattering (WSSUS) model proposed by Bello [1] is widely accepted as an adequate model for small-scale mobile fading channels [2]–[7]. A variety of standardized channel models for wireless and mobile communication systems has actually been developed on the basis of this stochastic model [8]–[13]. In order to obtain realizable and well specified representations of WSSUS channels, one often has to resort in practice to the use of simulation models (SMs). Different types of SMs can be used for the simulation of WSSUS channels, e.g., [15], [14]. However, a fundamental requirement for any of such SMs is the proper emulation of the essential characteristics of the WSSUS model. This characteristic is necessary to allow for a reliable and reproducible system performance investigation.

Several SMs basing on the time-variant tapped-delay-line (TDL) filter concept have been proposed to enable the implementation of WSSUS channels with continuous-time impulse responses, such as those in [5] and [15]. Among them, the simplest and perhaps most popular one is a so-called symbol-spaced TDL (SSTDL) model. Briefly speaking, a SSTDL model can be considered as a sampled version of the time-variant channel impulse response (CIR) obtained by using a sampling rate equal to the reciprocal of the symbol duration. Such kind of TDL models were originally introduced by Kailath [17] and Bello [1] as canonical channel models — which essentially are channel SMs — for band-limited time-variant linear (TVL) systems. SSTDL models are nowadays widely in use for evaluating the performance of modern wireless communication systems, e.g., [18]–[20].

It might seem that the applicability of SSTDL models is unquestionable, since they were developed in the framework of the sampling theorem [1]. Nonetheless, the results reported in [21] suggest that the pertinence of such TDL models is rather doubtful when the concept is applied to WSSUS channels. In fact, the answer to the question whether SSTDL models are suitable for modeling WSSUS channels is still lacking in the literature. What is more, despite

the fact that this modeling approach dates back more than forty years [1], [17], the statistical properties of the resulting SSTDL are not well known. Most of the literature on this topic concentrates only on describing the structure of the SSTDL model [6], [7], and even though a statistical analysis can be found in [1], [4] and [16], no information concerning the channel frequency correlation function (FCF) is provided there. The information about the FCF is very important because this function influences the performance of many wide-band and frequency diversity wireless communication systems, such as multicarrier code division multiple access (MC-CDMA) systems [18]–[20], [22], [23].

Closing the above mentioned gaps is necessary not only for a better understanding of channel modeling aspects, but also for carrying out a reliable system performance investigation. In this paper, we aim at closing them by analyzing the pertinence and statistical behavior of SSTDL models for WSSUS channels. It is also our objective to discuss the problems associated with these TDL models, as well as to present a simple and effective strategy to avoid them.

The rest of the paper is organized as follows. Section 2 is committed to the analysis of the suitability of SSTDL models for simulating WSSUS channels. It is shown in Section 2 that using SSTDL models to model the CIR of WSSUS channels within the context of band-limited systems results in a violation of the channel's uncorrelated scattering (US) condition. In Section 3, we provide a concise description of the statistical behavior of these SMs. We show in that section that SSTDL models suffer from strong limitations in emulating the FCF of WSSUS channels. In Section 4, we show that SSTDL models lead to an imprecise performance evaluation of wireless communication systems sensitive to the FCF. To cope with this problem, we discuss a solution in Section 5 by doubling the sampling rate of the channel, resulting in a half-symbol-spaced TDL model. The usefulness of this solution is exemplary demonstrated by analyzing bit error probabilities for a down-link MC-CDMA system. Finally, we present our conclusions in Section 6.

2 About the Pertinence of SSTDL Models

2.1 The SSTDL Modeling Approach

Before analyzing the suitability of SSTDL models for modeling WSSUS channels, it is convenient to review the approach followed in [1] to obtain such SMs. Toward that end, consider a wireless communication system characterized by the input-output relationship

$$y(t) = x(t) * h(t,\tau) = \int x(t)h(t,\tau)d\tau \tag{1}$$

where $*$ denotes convolution, $x(t)$ is the transmitted signal, $y(t)$ is the received signal, and $h(t,\tau)$ is the time-variant CIR, which is continuous in both t and τ variables. The CIR $h(t,\tau)$, called input delay-spread function by Bello, may be regarded as being the system response at time t to a unit impulse applied τ seconds in the past.

For practical purposes, it is possible to derive discrete-delay[1] representations of the CIR $h(t,\tau)$ on the basis of the sampling theorem by assuming that either the transmitted signal or the channel itself is bandwidth restricted. For the latter case, it was shown in [1, pp. 378-379] that if the corresponding channel transfer function $H(t,f) \triangleq \int h(t,\tau)\exp\{-j2\pi f\tau\}d\tau$ is confined to a bandwidth $\mathcal{W}$ (meaning that $H(t,f) = 0$ for $|f| > \mathcal{W}$), then, according to the sampling theorem, the CIR $h(t,\tau)$ may equivalently be expressed as [1, eq. (123)]

$$h(t,\tau) \equiv \sum_{n=-\infty}^{\infty} h\left(t, \frac{n}{W}\right) \mathrm{sinc}\left(W\left[\tau - \frac{n}{W}\right]\right) \tag{2}$$

where $\mathrm{sinc}(\tau) \triangleq \sin(\pi\tau)/(\pi\tau)$, $W \geq \mathcal{W}$ is an arbitrary sampling rate, and $\delta(\tau)$ is the Dirac delta function.

In conformity with the thesis in [1], it turns out that the CIR $h(t,\tau)$ is well modeled by a

[1] In this paper, we will be concerned only with the discrete-delay modeling of the CIR $h(t,\tau)$. The reader is referred to [3] for a detailed study on the modeling of $h(t,\tau)$ in discrete-time domain

TDL linear filter having a time-variant impulse response

$$\hat{h}(t,\tau) = \Delta\tau \cdot \sum_{n=-\infty}^{\infty} h(t, n\Delta\tau)\delta(\tau - n\Delta\tau) \tag{3}$$

where the tap spacing $\Delta\tau \triangleq 1/W$ is given such that $\Delta\tau \leq 1/\mathcal{W}$. The equivalent discrete-delay CIR described by $\hat{h}(t,\tau)$ establishes the so-called SSTDL model when $W = \mathcal{W} = W_s$, where $W_s = 1/T$ is the nominal bandwidth of the transmitted symbols[2], and T is usually equal to the symbol duration[3]. We will refer through the paper to $\hat{h}(t,\tau)$ either as SSTDL model or as T-spaced TDL model to stress the fact that $\Delta\tau = T$ ($W_s = \mathcal{W} = W$), while we will use the term $\Delta\tau$-spaced TDL model for the more general case where $\Delta\tau \leq T$ ($W_s \leq \mathcal{W} \leq W$).

The equivalence between the CIR $h(t,\tau)$ and its discrete-delay version defined by $\hat{h}(t,\tau)$ in (3) holds in the sense that the former impulse response can be reconstructed from the interpolation of the latter one, as indicated by (2).

2.2 The Pertinence of SSTDL Models

The SSTDL modeling approach may at first seem to be sound and thorough. Nevertheless, important problems arise when the random nature of mobile fading channels is brought into consideration. The main source of conflict comes from the fact that the SSTDL model was derived on the basis of the sampling theorem for deterministic signals. If the CIR $h(t,\tau)$ is deemed to be a random process, as it is done usually for wireless communication system, it is obvious that its discrete-delay representation should instead be obtained by invoking the sampling theorem for stochastic processes [7, p. 71]. Thus, the bandwidth restriction should not

[2]The nominal bandwidth may be defined as the width of the main lobe of the power spectral density of a digitally modulated signal.

[3]For instance, T equals the duration of the quadrature-amplitude-modulation (QAM) symbols in a conventional single carrier system, whereas T equals the chip duration in direct-sequence spread spectrum (DS-SS) systems [23]. Multicarrier systems [23], [27] are a special case, where T is equal to the (non-cyclic-extended) symbol duration divided by the total number of subcarriers. In all cases, $W_s = 1/T$ holds. We note that the term "symbol" is used in this paper for those digital signals that carry the information through the channel.

be associated with the channel transfer function $H(t, f)$, but with the power density spectrum of $h(t, \tau)$. Fortunately, the amendment of such an imprecision results in the same equivalent discrete-delay CIR as described by $\hat{h}(t, \tau)$ in (3), and the results and conclusions drawn in [1] remain basically unchanged. In this case, however, the equivalence defined in (2) holds true only in the zero-mean-square-error sense, which signifies that [7, p. 71]

$$E\left\{\left|h(t,\tau) - \sum_{n=-\infty}^{\infty} h\left(t, \frac{n}{W}\right) \operatorname{sinc}\left(W\left[\tau - \frac{n}{W}\right]\right)\right|^2\right\} = 0 \tag{4}$$

where $E\{\cdot\}$ denotes statistical expectation. As cautioning remark, we point out that the sampling theorem for stochastic processes applies only on stationary processes.

A further problem appears if the CIR $h(t, \tau)$ meets per definition the WSSUS condition. If $h(t, \tau)$ is a WSSUS random process, then the simulation approach described in Section 2.1 is not applicable, because the US condition is incompatible with the bandwidth constraint presupposed to obtain $\hat{h}(t, \tau)$ [23]. Such an incompatibility often passes unnoticed in the literature. Take as an example the conclusions drawn in [7] at the end of Section 14.5.1 regarding the uncorrelatedness of the tap gains of $\hat{h}(t, \tau)$ being a consequence of the US condition of $h(t, \tau)$. This statement is not adequate in the way it was postulated in [7], because it was built on by implicitly assuming that the CIR $h(t, \tau)$ fulfills per definition both the WSSUS condition and the bandwitdh-limitation constrain. Notice that the eq. (14.5–4) given in [7, Sec. 14.5.1] holds true only if the channel transfer function is inherently band-limited.

Bello proposed a second TDL model which circumvents the incompatibility between the channel bandwidth limitation and the WSSUS condition [1, pp. 379, second column]. In deriving that model, Bello shifted the bandwidth constraint onto the input signal $x(t)$. Therefore, since the bandwidth restriction is external to the CIR $h(t, \tau)$, one can assume (without problems) that $h(t, \tau)$ is a WSSUS process. For this case, it can be shown that the equivalent

discrete-delay CIR is given by [16]

$$\tilde{h}(t,\tau) = \sum_{n=-\infty}^{\infty} \left[\int h(t,\xi)\mathrm{sinc}(W[\xi - n\Delta\tau])d\xi \right] \delta(\tau - n\Delta\tau). \tag{5}$$

The impulse response $\tilde{h}(t,\tau)$ is not equivalent to $h(t,\tau)$ in the sense of (2), but in what

$$y(t) \equiv \sum_{n=-\infty}^{\infty} x(t - n\Delta\tau) \int h(t,\xi)\mathrm{sinc}([\xi - n\Delta\tau])d\xi. \tag{6}$$

The previous equation implies that the output of the system remains the same if the CIR $h(t,\tau)$ is replaced by its discrete-delay version $\tilde{h}(t,\tau)$; as $y(t) = \tilde{y}(t)$, where $\tilde{y}(t) = x(t) * \tilde{h}(t,\tau)$. It is promptly seen that if $x(t)$ is random, then the equivalence $y(t) \equiv \tilde{y}(t)$ holds only in the zero-mean-square-error sense. Similar observations can be made for the SSTDL model, or more generally for the $\Delta\tau$-spaced TDL model, since $y(t) \equiv \hat{y}(t) * \mathrm{sinc}\,(Wt)$, where $\hat{y} = x(t) * \hat{h}(t,\tau)$.

While the TDL model described in (5) is compatible with WSSUS channels, it is strictly speaking not a valid SM for them. This is due to the fact that the tap gains of the equivalent discrete-delay CIR $\tilde{h}(t,\tau)$ are mutually correlated. The cross-correlation among the taps can nonetheless be neglected if the autocorrelation function of $h(t,\tau)$ varies slowly in the delay domain with respect to $\Delta\tau$, as pointed out in [1] and [16]. However, since the US condition of the CIR $h(t,\tau)$ is not well reflected in general by $\tilde{h}(t,\tau)$, it can be conclude that this SM is not adequate for modeling WSSUS channels. Indeed, the underlying reference model[4] of $\tilde{h}(t,\tau)$, which is a filtered version of $h(t,\tau)$, belongs to the class of non-WSSUS channels [24].

[4]In general, the reference model is any analytical model which specifies the statistical behavior of the simulated channel.

3 Statistical Behavior of SSTDL Models

Despite the SSTDL model proves to be incompatible with WSSUS channels from the perspective of band-limited systems, SMs of this kind are widely being used in connection with the WSSUS model to evaluate the performance of up-to-date wireless communication systems, e.g., [18]–[20]. In defense of such a system performance investigation approach, we can argue that the SSTDL model might coexist with WSSUS channels if the bandwidth constraint imposed on the CIR $h(t,\tau)$ is relaxed[5]. To find out if this is the case, it is necessary to know whether $\hat{h}(t,\tau)$ satisfactorily emulates the statistical properties of WSSUS channels. It should also be determined whether the resulting SSTDL model lends itself to system performance investigations. To accomplish the above-mentioned tasks, we need a complete description of the statistical behavior of the (nonequivalent) discrete-delay CIR $\hat{h}(t,\tau)$. In this section, we provide such a description by assuming that $h(t,\tau)$ is a WSSUS Gaussian random process. We will also assume that the CIR $h(t,\tau)$ is causal and has finite duration, so that

$$\hat{h}(t,\tau) = \Delta\tau \cdot \sum_{n=0}^{N} h(t, n\Delta\tau)\delta(\tau - n\Delta\tau) \tag{7}$$

where the number of taps $N \triangleq \lfloor W \cdot \tau_{\max} \rfloor + 1$ is defined with respect to the sampling rate W and the channel's maximum excess delay $\tau_{\max}$ [2]. The operator $\lfloor \cdot \rfloor$ denotes the nearest integer toward minus infinity. These assumptions will hold throughout the remaining of the paper.

3.1 Statistical Description of the Reference Channel Model

Before we proceed, we will summarize the statistical properties of the WSSUS Gaussian CIR $h(t,\tau)$ which are relevant for the purposes of this paper. For a detailed discussion on the

[5]Note, however, that the equivalences described in Section 2 for each of the pairs $\hat{h}(t,\tau)$, $h(t,\tau)$ and $\hat{y}(t)$, $y(t)$ will no longer be valid. In any case, the corresponding relationships between those functions should be established as mere approximations in terms of their statistical properties.

statistical properties of WSSUS channels we refer the reader to [1], [3], [7], and [23].

In line with the WSSUS Gaussian model, $h(t,\tau)$ is fully characterized by its autocorrelation function (ACF)

$$\begin{aligned} r_h(t_1,t_2;\tau_1,\tau_2) &\triangleq E\left\{h(t_1,\tau_1)h^*(t_2,\tau_2)\right\} \\ &= r_h(\Delta t;\tau_1)\delta(\tau_1-\tau_2) \end{aligned} \tag{8}$$

where $r_h(\Delta t;\tau) \triangleq E\{h(t,\tau)h^*(t+\Delta t,\tau)\}$, $\Delta t = t_1 - t_2$, and $\{\cdot\}^*$ denotes complex conjugate. Similarly, $h(t,\tau)$ can be completely characterized by its time-frequency ACF (TF-ACF)

$$\begin{aligned} R_H(t_1,t_2;f_1,f_2) &\triangleq E\left\{H(t_1,f_1)H^*(t_2,f_2)\right\} \\ &= \int\int r_h(t_1,t_2;\tau_1,\tau_2)\exp\{j2\pi(f_1\tau_1 - f_2\tau_2)\}d\tau_1 d\tau_2 \qquad (9) \\ &= R_H(\Delta t;\Delta f) \qquad (10) \end{aligned}$$

where $\Delta f = f_1 - f_2$. Equation (10) results from the substitution of $r_h(t_1,t_2;\tau_1,\tau_2)$ from (8) into (9), and states that the channel is wide-sense stationary[6] (WSS) in both the time and the frequency variables.

In particular, the multipath behavior of $h(t,\tau)$ is characterized in the frequency domain by the FCF $R_H(\Delta f) \triangleq R_H(0;\Delta f)$ and, equivalently, in the delay domain by the power delay profile (PDP)

$$\begin{aligned} S_\tau(\tau) &\triangleq E\{\|h(t,\tau)\|^2\} \\ &= \int_{-\infty}^{\infty} R_H(\Delta f)\mathrm{e}^{j2\pi\tau\Delta f}d\Delta f. \end{aligned} \tag{11}$$

We will focus our attention on these two statistical quantities (especially on the FCF) as the TDL models are mostly intended to emulate them [5].

[6]Actually, the channel is strict-sense stationary (SSS), since the underlying process is a Gaussian process.

3.2 Statistical Description of $\Delta\tau$-Spaced TDL Models

Given that $\hat{h}(t,\tau)$ is a sampled version of a Gaussian process, it is in turn a Gaussian process, which is therefore completely characterized by its ACF

$$\begin{aligned} r_{\hat{h}}(t_1,t_2;\tau_1,\tau_2) &= E\{\hat{h}(t_1,\tau_1)\hat{h}^*(t_2,\tau_2)\} \\ &= \frac{1}{W^2} r_h(\Delta t;\tau_1)\delta(\tau_1-\tau_2)\cdot\sum_{n=-\infty}^{\infty}\delta(\tau_1-nT) \end{aligned} \tag{12}$$

where $W \triangleq 1/\Delta\tau$. (We recall that $W = W_s$ for the T-spaced TDL model.) Equation (12) shows that $\hat{h}(t,\tau)$ is a WSSUS process, which was to be expected since the tap gains of $\hat{h}(t,\tau)$ are samples of a WSS random process that fulfills the US condition. We can therefore conclude that $\hat{h}(t,\tau)$ is an adequate SM for WSSUS channels. This is in line with the conclusion drawn in [7]. However, we came to it without presupposing any bandwidth limitation for the channel transfer function $H(t,f)$. In order to determine how accurate is this SM in emulating the statistical behavior of the reference model given by the CIR $h(t,\tau)$, it is convenient to turn our attention to the analysis of the FCF of $\hat{h}(t,\tau)$.

We can express the TF-ACF of $\hat{h}(t,\tau)$, denoted by $R_{\hat{H}}(t_1,t_2;f_1,f_2)$, as the convolution of the channel's TF-ACF $R_H(t_1,t_2;f_1,f_2) = R_H(\Delta t;\Delta f)$ and the train of delta functions $\sum_{n=-\infty}^{\infty}\delta(f_1-nW)/W$. In this way, we obtain

$$R_{\hat{H}}(t_1,t_2;f_1,f_2) = \frac{1}{W}\sum_{n=-\infty}^{\infty} R_H(\Delta t;\Delta f-nW) \tag{13}$$

$$= R_{\hat{H}}(\Delta t;\Delta f). \tag{14}$$

In turn, we can define the FCF of $\hat{h}(t,\tau)$ as $R_{\hat{H}}(\Delta f) \triangleq R_{\hat{H}}(0;\Delta f)$, i.e.,

$$R_{\hat{H}}(\Delta f) = \frac{1}{W}\sum_{n=-\infty}^{\infty} R_H(0;\Delta f-nW). \tag{15}$$

An equivalent expression which allows for the analytical evaluation of the FCF $R_{\hat{H}}(\Delta f)$ may be written as follows:

$$R_{\hat{H}}(\Delta f) = \frac{1}{W^2} \sum_{n=0}^{N} S_\tau(n/W) \exp\{-j2\pi n \Delta f / W\}. \tag{16}$$

We observe that $R_{\hat{H}}(t_1, t_2; f_1, f_2)$ is WSS in the time domain and wide-sense periodic in the frequency domain with period W. In mathematical terms, this means that $R_{\hat{H}}(t_1, t_2; f_1, f_2) = R_{\hat{H}}(\Delta t; \Delta f + kW)$, where k is an integer. Notice that $R_{\hat{H}}(\Delta f) = R_{\hat{H}}(\Delta f + kW)$. Also, the FCF $R_{\hat{H}}(\Delta \tau)$ is Hermitian symmetric, i.e., $R_{\hat{H}}(\Delta f) = R^*_{\hat{H}}(-\Delta f)$.

For an accurate emulation of the FCF $R_H(\Delta f)$ of the reference model it is desirable that $R_{\hat{H}}(\Delta f) = R_H(\Delta f)$. Nevertheless, this equality can be fulfilled only within the frequency interval $\Delta f \in [-W/2, W/2]$, because $R_{\hat{H}}(\Delta f) \neq R_H(\Delta f)$ for $|\Delta f| > W/2$ due to the periodicity of $R_{\hat{H}}(\Delta f)$. What is more, the FCF $R_{\hat{H}}(\Delta f)$ of the SM $\hat{h}(t, \tau)$ is a weighted sum of shifted replicas of $R_H(\Delta f)$, as can be observed from (15). Therefore, to ensure that the relation $R_{\hat{H}}(\Delta f) = R_H(\Delta f)$ holds for $\Delta f \in [-W/2, W/2]$, it is necessary that $R_H(\Delta f) = 0$ for $|\Delta f| > W/2$, otherwise the replicas of $R_H(\Delta f)$ will overlap and $R_{\hat{H}}(\Delta f)$ will be affected by aliasing. Unfortunately, the fulfillment of this condition cannot be guaranteed because the FCF of WSSUS channels is not band-limited, and $\hat{h}(t, \tau)$ does not include any external bandwidth restriction for $R_H(\Delta f)$ — which is actually the main difference between $\hat{h}(t, \tau)$ and the TDL model $\tilde{h}(t, \tau)$ described in Section 2. The FCF of $\hat{h}(t, \tau)$ will therefore be affected by a certain degree of aliasing, which will reduce its accuracy for emulating the FCF of $h(t, \tau)$. This is in fact the main drawback of the $\Delta\tau$-spaced TDL model. Owing to the aliasing effects, the FCF $R_{\hat{H}}(\Delta f)$ of $\hat{h}(t, \tau)$ provides just an approximation to the FCF $R_H(\Delta f)$ of the reference model $h(t, \tau)$ if $-W/2 \leq \Delta f \leq W/2$. Aliasing is a well-known effect, but to the best of the authors' knowledge, it is generally not recognized in the literature that this effect influences the statistical properties of the SM described by $\hat{h}(t, \tau)$ in (3).

On the other hand, a reliable performance analysis of wireless systems requires the accurate emulation of $R_H(\Delta f)$ along the whole frequency range of the system's bandwidth. Hence, satisfying the relation $R_{\hat{H}}(\Delta f) \approx R_H(\Delta f)$ within the interval $\Delta f \in [-W_s, W_s]$ is sufficient for system evaluation purposes. Unfortunately, this is not possible when we employ a T-spaced TDL model, because the period W of the FCF of this SM is equal to W_s, i.e., $W = W_s$, which means that the approximation $R_{\hat{H}}(\Delta f) \approx R_H(\Delta f)$ cannot be satisfied for $W_s/2 \leq |\Delta f| \leq W_s]$. As will be shown next, this characteristic of T-spaced TDL models seriously affects the performance evaluation of wireless communication systems sensitive to the FCF.

4 Numerical Examples

4.1 The Truncated-Exponential-Decay PDP

In this section, we will provide some examples to illustrate the issues discussed in Section 3.2. To this end, let us assume that the CIR $h(t, \tau)$ of the reference model has a truncated-exponential-decay (TED)-PDP

$$S_\tau(\tau) = \begin{cases} \frac{1}{c} \cdot e^{-\tau/\sigma}, & 0 \leq \tau \leq \tau_{\max} \\ 0, & \text{else} \end{cases} \tag{17}$$

where $\sigma > 0$ is called the PDP's falling factor, and $c = [1 - \exp\{-\tau_{\max}/\sigma\}]/\sigma$. The TED-PDP has been shown to be an adequate model for characterizing the PDP of outdoor and indoor wide-band channels [25]. Indeed, this type of PDP has been used as a reference for design and test by several bodies of standardization for wireless communication systems [8]–[10], [13], [26].

For the case of the TED-PDP, the FCF $R_H(\Delta f)$ of the reference model is given by

$$R_H(\Delta f) = \frac{1 - e^{-(1 - j2\pi\Delta f\sigma)\tau_{\max}/\sigma}}{(1 - j2\pi\Delta f\sigma) \cdot (1 - e^{-\tau_{\max}/\sigma})}. \tag{18}$$

From (16) and (17) we can express the FCF $R_{\hat{H}}(\Delta f)$ of the $\Delta\tau$-spaced TDL model $\hat{h}(t,\tau)$ as

$$R_{\hat{H}}(\Delta f) = \frac{1 - e^{-N(1+j2\pi\Delta f\sigma)/(W\sigma)}}{1 - e^{-(1+j2\pi\Delta f\sigma)/(W\sigma)}} \cdot \frac{1 - e^{-1/(W\sigma)}}{1 - e^{-N/(W\sigma)}}. \tag{19}$$

We normalized (16) to obtain the above expression, so that $R_{\hat{H}}(0) = 1$. Note that for the T-spaced TDL model, $R_{\hat{H}}(\Delta f)$ in (19) is periodic with $W = W_s$, i.e., $R_{\hat{H}}(\Delta f) = R_{\hat{H}}(\Delta f + kW_s)$.

4.2 Effects of Aliasing on the FCF

In Fig. 1, we present a comparison between $|R_{\hat{H}}(\Delta f)|$ and $|R_H(\Delta f)|$ for $\tau_{\max} = 800$ ns, $W = W_s = 20$ MHz, and three different values of the falling factor $\sigma = \{30 \text{ ns}, 60 \text{ ns}, 105 \text{ ns}\}$. These parameters are representative of the propagation conditions encountered inside office buildings ($\sigma = 30$ ns), at large open space environments ($\sigma = 60$ ns), and at outdoor environments under non-line of sight conditions ($\sigma = 105$ ns) [11] for applications in wireless local area networks (WLANs), such as HIPERLAN/2, where the system bandwidth W_s is equal to 20 MHz [10].

As can be seen in the three cases shown in Fig. 1, $|R_{\hat{H}}(\Delta f)|$ does not match $|R_H(\Delta f)|$ for the interval $\Delta f \in [-W_s/2, W_s/2]$, inside of which the approximation $R_{\hat{H}}(\Delta f) \approx R_{\hat{H}}(\Delta f)$ is valid. Actually, by taking the graphs of $|R_H(\Delta f)|$ as reference, we can observe that $|R_{\hat{H}}(\Delta f)|$ exhibits a correlation offset that increases monotonically as Δf moves from zero to $\pm W/2$. Since $R_H(\Delta f)$ is not bounded in the frequency domain, the above mentioned offset is indeed an effect caused by aliasing. We can also observe in Fig. 1 that $|R_{\hat{H}}(\Delta f)| \neq |R_H(\Delta f)|$ when $|\Delta f| > W/2$, as both FCFs clearly follow different trends for frequencies in excess of $W/2$.

4.3 The Influence of the FCF on the System Performance

Consider the frequency diversity system described by the following base-band equivalent signal model (we will assume that this system is free of inter-symbol interference (ISI))

$$\mathbf{Y} = \mathbf{C}\mathbf{X} + \mathbf{N} \tag{20}$$

where $\mathbf{X}$, $\mathbf{Y}, \mathbf{N} \in \mathbb{C}^{M\times 1}$ represent a vector of M transmitted signals, a vector of M received signals, and a vector of M complex additive white Gaussian noise (AWGN) components, respectively. The (n,n)th entry of the diagonal matrix $\mathbf{C} \in \mathbb{C}^{M\times M}$ represents the channel response of the nth transmitted signal centered at $(n-1)\cdot f_0$, where f_0 is the fundamental frequency of the system. The notation $\mathbb{C}^{m\times n}$ stands for the set of all $m \times n$ complex matrices.

Ideally, $\mathbf{C} = \text{diag}\{\mathbf{H}\}$, where the vector $\mathbf{H} \in \mathbb{C}^{M\times 1}$ represents the transfer function of the reference model $h(\tau;t)$ such that $\langle \mathbf{H}\rangle_n = H(n\Delta f;t)$ for all t. The diag$\{\cdot\}$ operator produces a diagonal matrix from a vector, where the diagonal elements of the matrix are equal to the elements of the vector between the curly braces; and $\langle\cdot\rangle_{n,m}$ denotes the entry of a matrix at its mth column and nth row (subindex m is omitted for vectors). Consequently, the channel correlation matrix $\mathbf{R_c} = E\{\mathbf{C}\mathbf{C}^*\}$ equals the reference correlation matrix $\mathbf{R} = E\{\mathbf{H}\mathbf{H}^H\}$, the (n,m)th entry of which is given as

$$\langle \mathbf{R}\rangle_{n,m} = R_H(W\cdot\Delta_{m-n}/M) \tag{21}$$

where $\Delta_{m-n} = m-n$ denotes the $(m-n)$th lag of $\mathbf{R}$, and $\{\cdot\}^H$ indicates the conjugate transpose operation.

When we use a T-spaced TDL model (or a $\Delta\tau$-spaced TDL model in general) for simulating the system described by (20), then the channel matrix $\mathbf{C}$ is equivalent to $\hat{\mathbf{C}} = \text{diag}\{\hat{\mathbf{H}}\}$, where

$\hat{\mathbf{H}} = \text{fft}\{\hat{\mathbf{h}}\}_{\tau \mapsto \Delta f}$, and $\hat{\mathbf{h}} \in \mathbb{C}^{M \times 1}$ with $M \geq N$ is the vector representation[7] of $\hat{h}(\tau; t)$. The notation $\text{fft}\{\cdot\}_{\tau \mapsto \Delta f}$ indicates the column-wise fast Fourier transform (FFT) of a matrix with respect to Δf. In this case, the correlation matrix $\mathbf{R_c}$ is equal to $\hat{\mathbf{R}}$, where $\hat{\mathbf{R}} = E\{\hat{\mathbf{H}}\hat{\mathbf{H}}^H\}$ is related to $R_{\hat{H}}(\Delta f)$ by

$$\langle \hat{\mathbf{R}} \rangle_{n,m} = R_{\hat{H}}(W \cdot \Delta_{m-n}/M). \tag{22}$$

It follows from (21) and (22) that

$$\langle \hat{\mathbf{R}} \rangle_{n,m} \approx \langle \mathbf{R} \rangle_{n,m}, \quad \text{for } |\Delta_{m-n}| \leq \lfloor M/2 \rfloor \tag{23}$$

$$\langle \hat{\mathbf{R}} \rangle_{n,m} \neq \langle \mathbf{R} \rangle_{n,m}, \quad \text{for } |\Delta_{m-n}| > \lfloor M/2 \rfloor \,. \tag{24}$$

By assuming binary phase shift keying (BPSK) modulation and maximal ratio combining (MRC), we can express the BEP of this system by [23, Sect. 2.4.6]

$$P_{BEP} = \frac{1}{\pi} \int_0^{\pi/2} \prod_{i=1}^{M} \left(\frac{1}{1 + \frac{E_b}{N_0} \cdot \frac{\lambda_i}{M \cdot \sin^2 \theta}} \right) d\theta \tag{25}$$

where E_b is the bit energy, N_0 is the noise density, and λ_i is the ith eigenvalue of the correlation matrix $\mathbf{R_c}$. From (25), and since the eigenvalues of $\mathbf{R}$ and $\hat{\mathbf{R}}$ are not exactly the same because of (23) and (24), the BEP of the reference system described by (20) will differ from that of the simulation system described by $\hat{\mathbf{Y}} = \hat{\mathbf{C}}\mathbf{X} + \mathbf{N}$, where $\hat{\mathbf{C}} = \text{diag}\{\hat{\mathbf{H}}\}$.

As a numerical example, let us analyze the BEP of a down-link MC-CDMA system [28] consisting of $M = 64$ orthogonal subcarriers with $f_0 = 312.5$ kHz, all of them used as data subcarriers. The nominal bandwidth of this system is $W_s = 20$ MHz ($W_s = 64 \times 312.5$ kHz),

[7] The elements of $\hat{\mathbf{h}}$ are given such that $\langle \hat{\mathbf{h}} \rangle_n$ equals the nth tap gain of $\hat{h}(\tau; t)$ for $n = 0, \ldots, N$; while $\langle \hat{\mathbf{h}} \rangle_n = 0$ for $n = N, \ldots, M-1$. In turn, the value of M is defined with respect to a given observation interval τ_{obs} in such a way that $M = \lceil \tau_{obs} \cdot W \rceil$ and $\tau_{obs} > \tau_{max}$. The operator $\lceil \cdot \rceil$ denotes the nearest integer toward infinity. Obviously, $\hat{\mathbf{h}}$ and $\hat{h}(\tau; t)$ describe equivalent SMs.

and $T = 1/W_s$ is therefore equal to 50 ns. We assume a multiple-user-interference (MUI)-free network scenario with BPSK and MRC, and we consider $M_{\mathrm{SF}} = \{1, 2, 4, 8, 16, 32, 64\}$, where M_{SF} denotes the spreading factor of the system ($M_{\mathrm{SF}} \leq M$). To compute the BEP for different spreading factors, we used a slightly modified version of (25), which is given by

$$P_{BEP-SF} = \frac{1}{\pi} \int_0^{\pi/2} \prod_{i=1}^{M_{\mathrm{SF}}} \left(\frac{1}{1 + \frac{E_b}{N_0} \cdot \frac{\tilde{\lambda}_i^{(M_{\mathrm{SF}})}}{M_{\mathrm{SF}} \cdot \sin^2\theta}} \right) d\theta \tag{26}$$

where $\tilde{\lambda}_i^{(M_{\mathrm{SF}})}$ is the ith eigenvalue of the submatrix $\mathbf{R}_{\mathbf{c}}^{(M_{\mathrm{SF}})} \in \mathbb{C}^{M_{\mathrm{SF}} \times M_{\mathrm{SF}}}$, the (n, m)th entry of which is $\langle \mathbf{R}_{\mathbf{c}}^{(M_{\mathrm{SF}})} \rangle_{n,m} = \langle \mathbf{R}_{\mathbf{c}} \rangle_{n,m}$. We evaluated (26) considering the T-spaced TDL model and the TED-PDP [see (17)] with $\tau_{max} = 800$ ns and the same values of the falling factor σ considered for Fig. 1. The results obtained for $\sigma = 30$ ns are shown in Fig. 2, while the results obtained for $\sigma = 60$ ns and $\sigma = 105$ ns are presented in Fig. 3 and Fig. 4, respectively.

As can be seen in Figs. 2, 3, and 4, the BEP of the reference system $\mathbf{Y} = \mathbf{C}\mathbf{X} + \mathbf{N}$ with $M_{\mathrm{SF}} > 1$ is not exactly the same as that of the simulation system $\hat{\mathbf{Y}} = \hat{\mathbf{C}}\mathbf{X} + \mathbf{N}$. In fact, the difference between the BEP of both systems increases with increasing the spreading factor M_{SF}. This is because the approximation $\hat{\mathbf{R}}^{(M_{\mathrm{SF}})} \approx \mathbf{R}^{(M_{\mathrm{SF}})}$ is worse due to the aliasing effects as M_{SF} increases — The submatrices $\hat{\mathbf{R}}^{(M_{\mathrm{SF}})}, \mathbf{R}^{(M_{\mathrm{SF}})} \in \mathbb{C}^{M_{\mathrm{SF}} \times M_{\mathrm{SF}}}$ are given such that $\langle \hat{\mathbf{R}}^{(M_{\mathrm{SF}})} \rangle_{n,m} = \langle \hat{\mathbf{R}} \rangle_{n,m}$ and $\langle \mathbf{R}^{(M_{\mathrm{SF}})} \rangle_{n,m} = \langle \mathbf{R} \rangle_{n,m}$. Interestingly, Fig. 4 shows that the aliasing effects can be neglected if σ is large. This was to be expected, since the FCF $R_H(\Delta f)$ of $h(t, \tau)$ decays fast for large values of σ [cf. Fig. 1], which enhances the quality of the approximation defined in (23). However, the BEP of $\hat{\mathbf{Y}} = \hat{\mathbf{C}}\mathbf{X} + \mathbf{N}$ is clearly different from that of $\mathbf{Y} = \mathbf{C}\mathbf{X} + \mathbf{N}$ when $M_{\mathrm{SF}} = 64$ even for a large σ, because half of the elements in $\hat{\mathbf{R}}^{(64)}$ do not meet the relation $\langle \hat{\mathbf{R}}^{(64)} \rangle_{m,n} \approx \langle \mathbf{R}^{(64)} \rangle_{m,n}$ [see (24)].

5 Avoiding the Problems Caused by T-Spaced TDL Models

SSTDL models lead to an imprecise system performance evaluation because of two reasons. On the one hand, the quality of the relation $R_{\hat{H}}(\Delta f) \approx R_H(\Delta f)$, $\Delta f \in [-W_s/2, W_s/2]$, is affected by aliasing effects. On the other hand, $R_{\hat{H}}(\Delta f) \neq R_H(\Delta f)$ for $\Delta f \notin [-W_s/2, W_s/2]$ since $R_{\hat{H}}(\Delta f)$ behaves different from $R_H(\Delta f)$ when $|\Delta f| > W_s/2$. Fortunately, these problems can be solved, or at least sufficiently reduced, simply by increasing the sampling rate of the channel, i.e., by reducing the tap spacing $\Delta\tau$ in $\hat{h}(\tau; t)$.

Reducing $\Delta\tau$ will result in less severe aliasing effects provided that $R_H(\Delta f) \longrightarrow 0$ as $\Delta f \longrightarrow \pm\infty$ (most PDPs, including the TED-PDP in (17), meet this condition). In addition, it is obvious from (15) that a higher sampling rate results in a larger period for $R_{\hat{H}}(\Delta f)$ and, consequently, in a larger approximation interval. Indeed, it can be shown that $R_{\hat{H}}(\Delta f) \longrightarrow R_H(\Delta f)$ as $\Delta\tau \longrightarrow 0$. Particularly, if we choose $\Delta\tau = T/2$, then the period W of $R_{\hat{H}}(\Delta f)$ will be conveniently equal to twice W_s, i.e., $W = 2W_s$. In this way, the approximation $R_{\hat{H}}(\Delta f) \approx R_H(\Delta f)$ will hold for the relevant interval $\Delta f \in [-W_s, W_s]$. As a result, we will obtain a more reliable picture of the system's performance while keeping the TDL model's complexity low. For the above mentioned reasons, we suggest to sample the CIR at a rate equal to twice W_s as alternative to avoid the problems associated to T-spaced TDL models. For the sake of clarity, we will henceforth refer to the oversampled TDL model having a tap spacing of $\Delta\tau = T/2$ as the $T/2$–spaced TDL model.

Figure 5 illustrates the advantages of using $T/2$-spaced TDL models by comparing the absolute value of the FCF of the reference model, $|R_H(\Delta f)|$, with that of the T-spaced and $T/2$-spaced TDL models. As expected, this figure shows that $T/2$-spaced TDL models are more resilient to the aliasing effects than T-spaced TDL models. Furthermore, we can observe in Fig. 5 that the approximation interval of $T/2$-spaced TDL model is valid for $\Delta f \in [-W_s, W_s]$.

As a numerical example of the benefits of $T/2$-spaced TDL models for system evaluation, let us consider again the MC-CDMA system described in Section IV. We have recalculated the BEP of this system under the same considerations as in Section IV, but with the difference that we use now a $T/2$–spaced TDL channel model, meaning that the tap spacing is equal to $\Delta\tau = 25$ ns and $\hat{\mathbf{h}} \in \mathbb{C}^{128\times 1}$ with $N = 33$. The results are shown in Figs. 6, 7, and 8.

It is clear from Figs. 6, 7, and 8, that the simulation system $\hat{\mathbf{Y}} = \hat{\mathbf{C}}\mathbf{X} + \mathbf{N}$ matches better the BEP of the reference system $\mathbf{Y} = \mathbf{C}\mathbf{X} + \mathbf{N}$ when the $T/2$–spaced TDL channel model is used. Moreover, in the BEP curves of $\mathbf{Y}$ and $\hat{\mathbf{Y}}$ corresponding to a SF of 64, we can see that the difference between the graphs is considerably smaller than when we use the T–spaced TDL model (see Figs. 2, 3, and 4). The reason for this significant improvement is that the approximation $R_{\hat{H}}(\Delta f) \approx R_H(\Delta f)$ is valid for $\Delta f \in [-Ws, Ws]$ when we use a $T/2$-spaced TDL model. We shall mention, nonetheless, that the $T/2$-spaced TDL model has been introduced mainly as a solution to enable the approximation of the FCF $R_H(\Delta f)$ along the relevant range of frequencies of the system $-W_s \leq \Delta f \leq W_s$. It does not remove completely the aliasing effects observed within $\Delta f \in [-W/2, W/2]$, which explains the slight differences between the BEP of the reference system and the simulation system for $\sigma = 30$ ns and $M_{\mathrm{SF}} = 64$ [cf. Fig. 8]. Other solutions, more sophisticated than the one discussed here, are necessary to neutralize the aliasing effects, e.g., see [5].

6 Conclusions

We showed that important inconsistencies arise when SSTDL models, or $\Delta\tau$-spaced TDL models in general, are used within the context of band-limited systems to model WSSUS channels. Such inconsistencies involve the violation of the US condition of the channel. The $\Delta\tau$-spaced TDL model defined by $\hat{h}(t, \tau)$ is nevertheless a valid SM for WSSUS channels if it is considered out of the context of band-limited systems. This is because the resulting $\Delta\tau$-spaced

TDL model turns out to be in itself a WSSUS random process.

We have shown that the FCF $R_{\hat{H}}(\Delta f)$ of the $\Delta\tau$-spaced TDL models is periodic with a period equal to $W = 1/\Delta\tau$, which cause aliasing effects. Because of this characteristic of $R_{\hat{H}}(\Delta f)$, $\Delta\tau$-spaced TDL models provide just an approximation to the FCF $R_H(\Delta f)$ of the reference model $h(t,\tau)$, which is valid only for $\Delta f \in [-W/2, W/2]$. The quality of such an approximation is determined by the aliasing effects.

Given that the relation $R_{\hat{H}}(\Delta f) \approx R_H(\Delta f)$ is not valid for $|\Delta f| > W/2$, T-spaced TDL models are not able to emulate the FCF of the reference model for the frequency range of the system's bandwidth W_s (as $W = W_s$ for T-spaced TDL models). This drawback seriously affects the performance analysis of wireless communication systems sensitive to the FCF.

To avoid the problems caused by T-spaced TDL models, we suggested the use of $T/2$–spaced TDL channel models, which are obtained by sampling the CIR at a rate equal to $2W_s$, i.e., $\Delta\tau = T/2$. The $T/2$-spaced TDL model will be more resilient to the aliasing effects than the T-spaced TDL model provided that the FCF $R_H(\Delta f)$ of the reference model approaches to zero as $\Delta f \to \infty$. Another advantage is that $T/2$ spaced TDL models allow for the approximation of the FCF of the reference model along the complete frequency range of the system's bandwidth. For this reason, using $T/2$-spaced TDL models instead of T-spaced TDL models turns out to be of great advantage for system evaluation purposes.

References

[1] Bello PA. Characterization of randomly time-variant linear channels. *IEEE Trans. Commun. Syst.* 1963; **CS-11**: 360-393.

[2] Sklar B. *Digital communications: Fundamentals and Applications*. Prentice-Hall: Englewood Cliffs, NJ, 1988.

[3] Pätzold M. *Mobile Fading Channels*. John Wiley & Sons: Chichester, UK, 2002.

[4] Jeruchim MC, Balaban P, Shanmugan KS, 2nd ed. *Simulation of Communication Systems: Modeling, Methodology, and Techniques*. Kluwer: Berlin, Germany, 2000, ch. 9.

[5] Pätzold M, Szczepanski A, Youssef N. Methods for modeling of specified and measured multipath power-delay profiles. *IEEE Trans. Veh. Tech.* 2002; **51(5)**: 978-988.

[6] Stein S. Fading channel issues in system engineering. *IEEE J. Select. Areas Commun.* 1987; **SAC-5(2)**: 68-89.

[7] Proakis JG. 4th ed. *Digital Communications*. McGraw-Hill: New York, 2001, ch. 14.

[8] COST 207. Digital land mobile radio communications. Office Official Publ. Eur. Communities, Final Rep. Luxemburg, 1989.

[9] ETSI. Radio Transmission and Reception. ETSI. GSM 05.05. ETSI EN 300 910 V8.5.1, 2000.

[10] ETSI. Broadband radio access networks (BRAN), HIPERLAN Type2 Technical specification: Physical layer. *Ots/bran 0023003*, ETSI; October 1999.

[11] Medbo J, Berg JE. Measured radio wave propagation characteristics at 5 GHz for typical HIPERLAN/2 scenarios. *Tech. Rep. 3ERI074a, ETSI*; Sophia-Antipolis, France, 1998.

[12] Medbo J, Schramm P. Channel models for HIPERLAN/2. *Tech. Rep. 3ERI085B, ETSI*; Sophia-Antipolis, France, 1998.

[13] Erceg V, et al. TGn channel models. *Tech. Rep. IEEE P802.11, Wireless LANs*; Garden Grove, Calif, USA, 2004.

[14] Chryssomallis M. Simulation of mobile fading channels. *IEEE Antennas and Propagation Magazine.* 2002; **44(6)**: 172-183.

[15] Yip KW, Ng TS. Efficient simulation of digital transmission over WSSUS channels. *IEEE Trans. Commun.* 1995; **43(12)**: 2907-2913.

[16] Sykora J. Tapped delay line model of linear randomly time-variant WSSUS channel. *Electron. Lett.* 2000; **36(19)**: 1656-1657.

[17] Kailath T. Sampling models for linear time-variant filters. *Report No. 352*; M.I.T. Research Lab. of Electronics, Cambridge, Mass, May 1959.

[18] Choi YS, Voltz PJ, Cassara FA. On channel estimation and detection for multicarrier signals in fast and selective Rayleigh fading channels. *IEEE Trans. Commun.* 2001; **49(8)**: 1375-1387.

[19] Yang LL, Hanzo L. Performance of generalized multicarrier DS-CDMA over Nakagami-m fading channels. *IEEE Trans. Commun.* 2002; **50(6)**: 956-966.

[20] Hou Z, Dubey VK. Exact analysis for downlink MC-CDMA in Rayleigh fading channels. *IEEE Commun. Lett.* 2004; **8(2)**: 90-92.

[21] Gutierrez CA, Cabrera M. Issues of the Simulation of Wireless Channels with Exponential-Decay Power-Delay Profiles. In *Proc. of the 16th IEEE International Symposium on Personal, Indoor, and Mobile Radio Communications, IEEE PIMRC 2005*, Berlin, Germany, Sept. 2005; pp. 507-511.

[22] Hara S, Prasad R. Overview of Multicarrier CDMA. *IEEE Commun. Mag.* 1997; **35(12)**: 126-133.

[23] Schulze H, Lüders C. *Theory and Applications of OFDM and CDMA.* John Wiley & Sons, 2005, ch. 2.

[24] Matz G. On non-WSSUS wireless fading channels. *IEEE Trans. Wireless Commun.* 2005; **4(5)**: 2465-2478.

[25] Erceg V, et al. A model for the multipath delay profile of fixed wireless channels. *IEEE J. Select. Areas Commun.* 1999; **17(3)**: 399-410.

[26] Correia LM, Ed. *Wireless Flexible Personalised Communications (COST 259 Final Report).* John Wiley & Sons: Chichester, UK, 2001.

[27] van Nee R, Prasad R. *OFDM for Wireless Multimedia Communications.* Artech House, 2004.

[28] Gutierrez CA, Sanchez J, Cabrera M, Gutierrez L. MC-CDMA based architecture for the downlink of infrastructure WLANs. In *Proc. of the 17th IEEE International Symposium on Personal, Indoor, and Mobile Radio Communications, IEEE PIMRC 2006*, Helsinki, Finland, Sept. 2006.

Authors Vitae

Carlos-Adrián Gutiérrez-Díaz-de-León received the B.E. degree from the Autonomous University of Aguascalientes, Ags., México, in 2002, and the M.S. degree from the Scientific Research and Higher Education Center of Ensenada (CICESE), BC, México, in 2006, both in electrical engineering with major on telecommunications. He also received the Advanced Studies Diploma (DEA) from the Polytechnic University of Catalonia (UPC), Barcelona, Spain, in 2005. He is an Assistant Professor (currently on a leave) of Electrical Engineering at the Panamericana University, Campus Bonaterra, Ags., México, and a Doctorate Fellow at the Faculty of Engineering and Science, Agder University College, Grimstad, Norway. His research interests include modeling and simulation of mobile fading channels for SISO and MIMO systems, and physical layer aspects of OFDM and MC-CDMA systems.

Margarita Cabrera-Bean received the Electrical Engineering degree and the Ph D. from the Polytechnic University of Catalonia (UPC), Barcelona, Spain. She is an Associate Professor at the Polytechnic University of Catalonia, Barcelona, Spain, where she teaches undergraduate courses in analog and digital communications and graduate courses in signal processing. Her current research interests are in general signal processing applications and include mobile communication systems, MIMO and SISO channel models, spatial diversity, Code Division Multiple Access (CDMA), and pattern recognition.

Matthias Pätzold received the Dipl.-Ing. and Dr.-Ing. degrees in electrical engineering from Ruhr-University Bochum, Bochum, Germany, in 1985 and 1989, respectively, and the habil. degree in communications engineering from the Technical University of Hamburg-Harburg, Hamburg, Germany, in 1998. From 1990 to 1992, he was with ANT Nachrichtentechnik GmbH, Backnang, Germany, where he was engaged in digital satellite communications. From 1992 to 2001, he was with the Department of Digital Networks at the Technical University Hamburg-Harburg. Since 2001, he has been a full professor of mobile communications with Agder University College, Grimstad, Norway. He is author of the books "Mobile Radio Channels - Modelling, Analysis, and Simulation" (in German) (Wiesbaden, Germany: Vieweg, 1999) and "Mobile Fading Channels" (Chichester, U.K.: Wiley & Sons, 2002). His current research interests include mobile radio communications, especially multipath fading channel modelling, multi-input multi-output (MIMO) systems, channel parameter estimation, and coded-modulation techniques for fading channels.

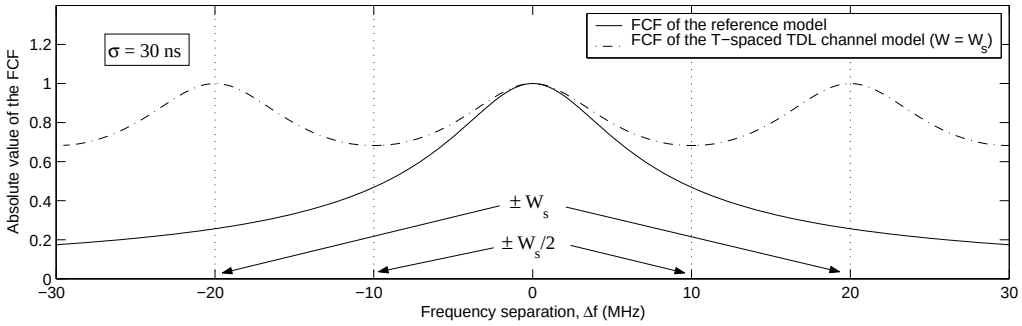

(a)

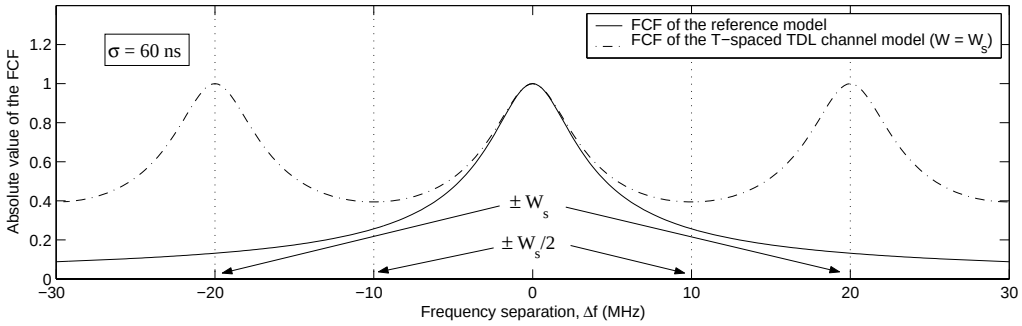

(b)

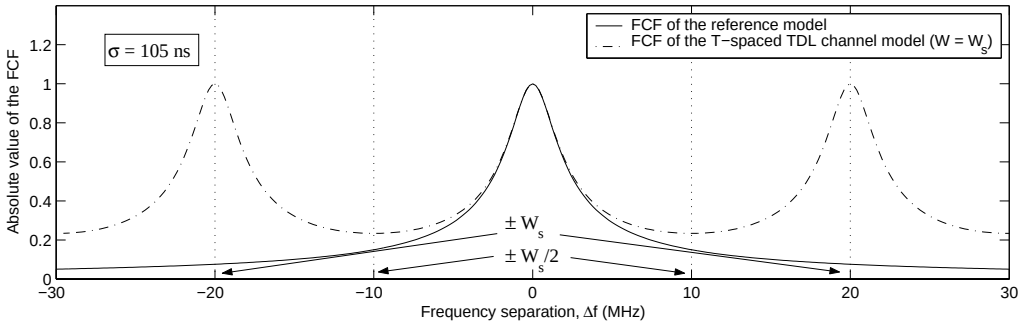

(c)

Figure 1: Comparison between $|R_H(\Delta f)|$ and $|R_{\hat{H}}(\Delta f)|$ by using the T-spaced TDL model, by assuming the TED-PDP with $\tau_{\max} = 800$ ns, $W_s = 20$ MHz ($W = W_s$), and $\sigma = \{30 \text{ ns}, 60 \text{ ns}, 105 \text{ ns}\}$.

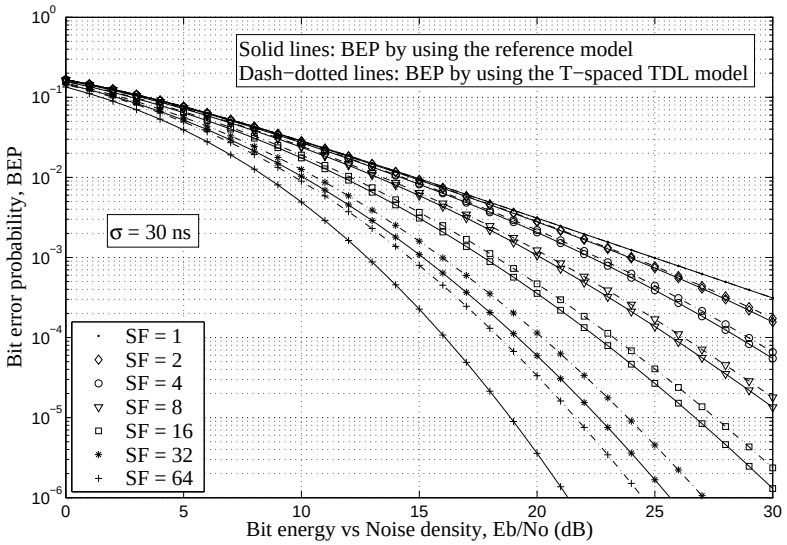

Figure 2: Bit error probabilities (BEPs) of an MUI-free down-link MC-CDMA system with MRC and different values of the spreading factor M_{SF}. Solid lines: BEPs of the reference system $\mathbf{Y} = \mathbf{CX}+\mathbf{N}$, which were computed by using the reference channel model $\mathbf{C} = \mathrm{diag}\{\mathbf{H}\}$. Dash–dotted lines: BEPs of the simulation system $\hat{\mathbf{Y}} = \hat{\mathbf{C}}\mathbf{X} + \mathbf{N}$, which were computed by using the vector representation of the T-spaced TDL model $\hat{\mathbf{C}} = \mathrm{diag}\{\hat{\mathbf{H}}\}$.

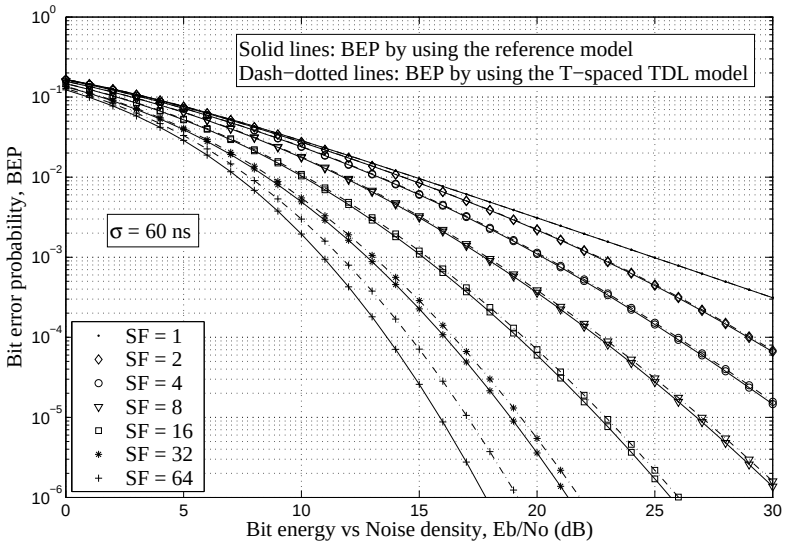

Figure 3: Bit error probabilities (BEPs) of an MUI-free down-link MC-CDMA system with MRC and different values of the spreading factor M_{SF}. Solid lines: BEPs of the reference system $\mathbf{Y} = \mathbf{CX}+\mathbf{N}$, which were computed by using the reference channel model $\mathbf{C} = \mathrm{diag}\{\mathbf{H}\}$. Dash–dotted lines: BEPs of the simulation system $\hat{\mathbf{Y}} = \hat{\mathbf{C}}\mathbf{X} + \mathbf{N}$, which were computed by using the vector representation of the T-spaced TDL model $\hat{\mathbf{C}} = \mathrm{diag}\{\hat{\mathbf{H}}\}$.

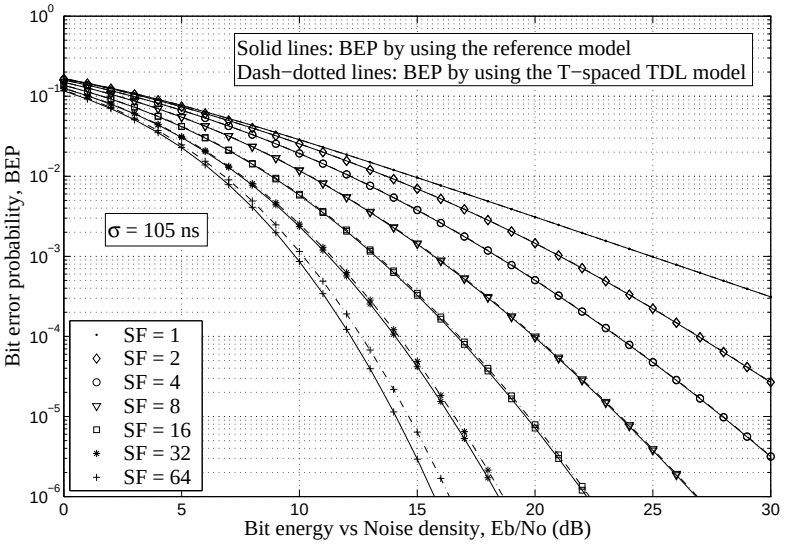

Figure 4: Bit error probabilities (BEPs) of an MUI-free down-link MC-CDMA system with MRC and different values of the spreading factor M_{SF}. Solid lines: BEPs of the reference system $\mathbf{Y} = \mathbf{C}\mathbf{X}+\mathbf{N}$, which were computed by using the reference channel model $\mathbf{C} = \mathrm{diag}\{\mathbf{H}\}$. Dash–dotted lines: BEPs of the simulation system $\hat{\mathbf{Y}} = \hat{\mathbf{C}}\mathbf{X} + \mathbf{N}$, which were computed by using the vector representation of the T-spaced TDL model $\hat{\mathbf{C}} = \mathrm{diag}\{\hat{\mathbf{H}}\}$.

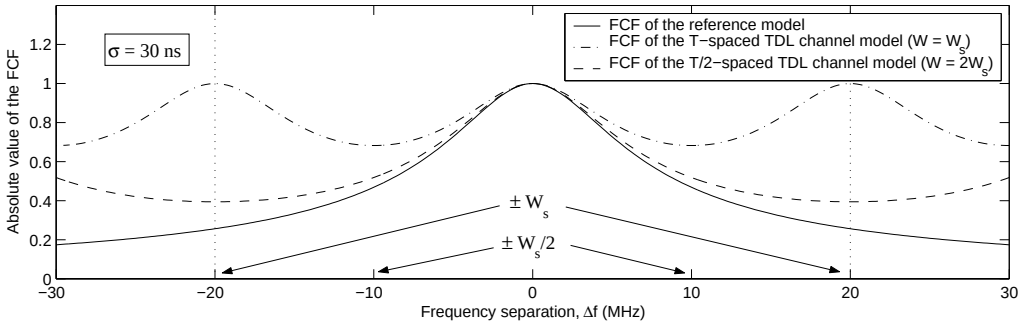

(a)

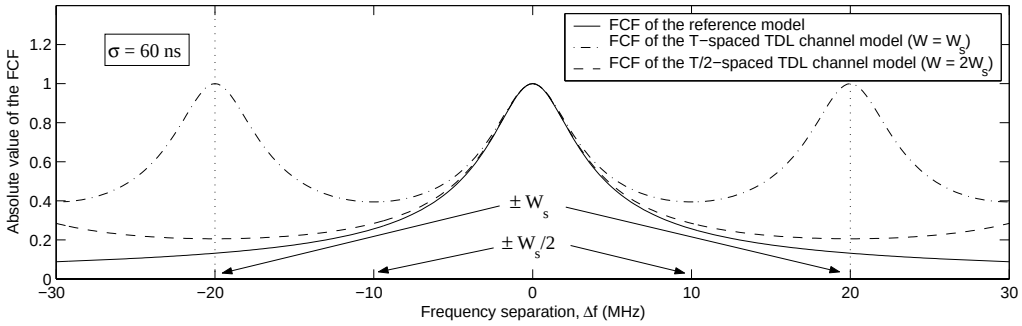

(b)

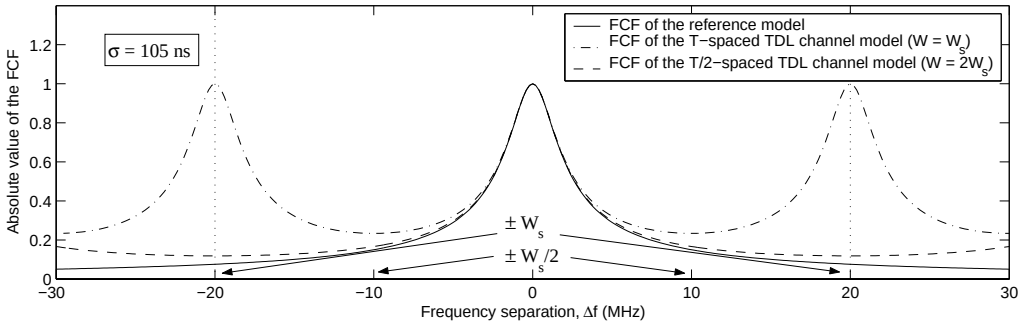

(c)

Figure 5: Comparison between $|R_H(\Delta f)|$ and $|R_{\hat{H}}(\Delta f)|$ by using the T-spaced TDL model (dashed lines) and the $T/2$-spaced TDL model (dotted lines) by assuming the TED-PDP with $\tau_{\max} = 800$ ns, $W_s = 20$ MHz, and $\sigma = \{30 \text{ ns}, 60 \text{ ns}, 105 \text{ ns}\}$.

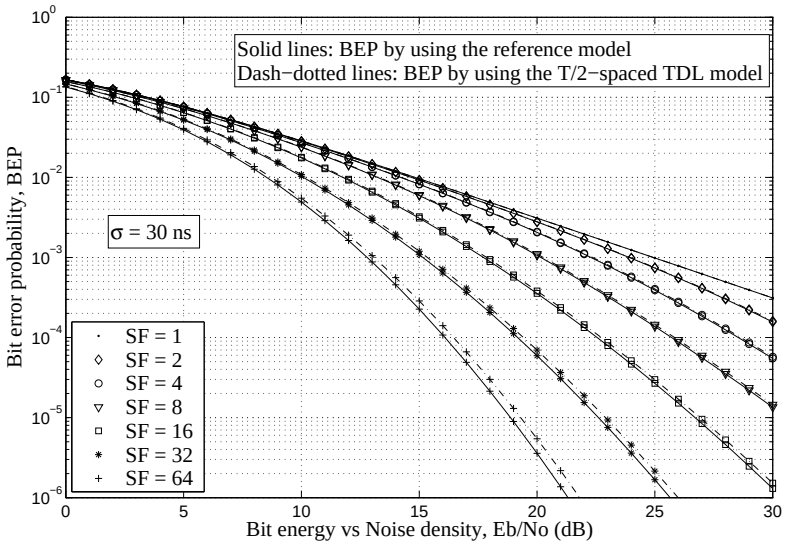

Figure 6: Bit error probabilities (BEPs) of an MUI-free down-link MC-CDMA system with MRC and different values of the spreading factor M_{SF}. Solid lines: BEPs of the reference system $\mathbf{Y} = \mathbf{CX}+\mathbf{N}$, which were computed by using the reference channel model $\mathbf{C} = \mathrm{diag}\{\mathbf{H}\}$. Dash–dotted lines: BEPs of the simulation system $\hat{\mathbf{Y}} = \hat{\mathbf{C}}\mathbf{X} + \mathbf{N}$, which were computed by using the vector representation of the $T/2$-spaced TDL model $\hat{\mathbf{C}} = \mathrm{diag}\{\hat{\mathbf{H}}\}$.

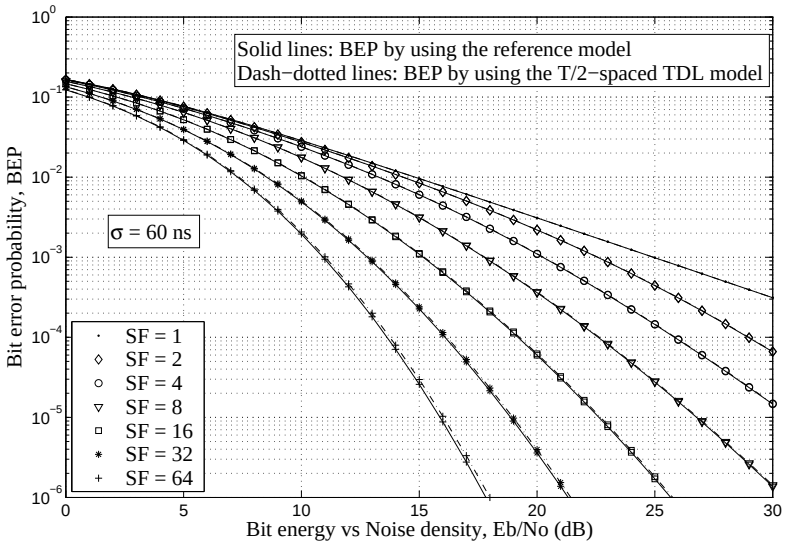

Figure 7: Bit error probabilities (BEPs) of an MUI-free down-link MC-CDMA system with MRC and different values of the spreading factor M_{SF}. Solid lines: BEPs of the reference system $\mathbf{Y} = \mathbf{CX}+\mathbf{N}$, which were computed by using the reference channel model $\mathbf{C} = \mathrm{diag}\{\mathbf{H}\}$. Dash–dotted lines: BEPs of the simulation system $\hat{\mathbf{Y}} = \hat{\mathbf{C}}\mathbf{X} + \mathbf{N}$, which were computed by using the vector representation of the $T/2$-spaced TDL model $\hat{\mathbf{C}} = \mathrm{diag}\{\hat{\mathbf{H}}\}$.

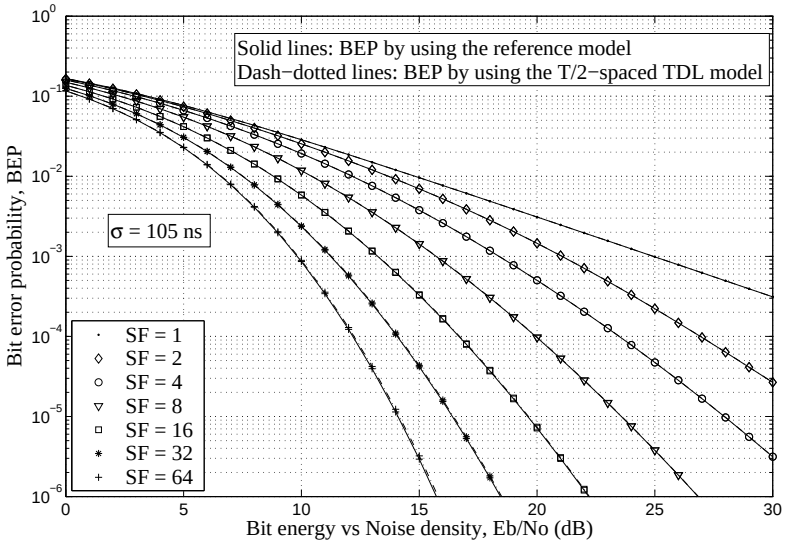

Figure 8: Bit error probabilities (BEPs) of an MUI-free down-link MC-CDMA system with MRC and different values of the spreading factor M_{SF}. Solid lines: BEPs of the reference system $\mathbf{Y} = \mathbf{CX}+\mathbf{N}$, which were computed by using the reference channel model $\mathbf{C} = \mathrm{diag}\{\mathbf{H}\}$. Dash–dotted lines: BEPs of the simulation system $\hat{\mathbf{Y}} = \hat{\mathbf{C}}\mathbf{X} + \mathbf{N}$, which were computed by using the vector representation of the $T/2$-spaced TDL model $\hat{\mathbf{C}} = \mathrm{diag}\{\hat{\mathbf{H}}\}$.